International Journal of Thermal Sciences 49 (2010) 786–796

Contents lists available at ScienceDirect

International Journal of Thermal Sciences

journal homepage: www.elsevier.com/locate/ijts

Numerical study of compressible convective heat transfer with variations in all fluid properties

Nitin P. Gulhane, Shripad P. Mahulikar*

Department of Aerospace Engineering, Indian Institute of Technology Bombay, P.O. IIT Powai Mumbai 400076, India

ARTICLE INFO

Article history:
Received 15 February 2009
Received in revised form
24 October 2009
Accepted 1 November 2009
Available online 28 November 2009

Keywords:
Axial conduction
Micro-flow
Radial convection
Variable fluid properties

ABSTRACT

The effects of property variations in single-phase laminar forced micro-convection with constant wall heat flux boundary condition are investigated in this work. The fully-developed flow through micro-sized circular (axisymmetric) geometry is numerically studied using two-dimensional continuum-based conservation equations. The non-dimensional governing equations show significance of momentum transport in radial direction due to $\mu(T)$ variation and energy transport by fluid conduction due to $k(T)$ variation. For the case of heated air, variation in $C_p(T)$ and $k(T)$ causes increase in Nu. This is owing to: (i) reduction in T_w, $(T_w - T_m)$, and $(\partial T/\partial r)_w$ and (ii) change in $\partial T_m/\partial z$ results in axial conduction along the flow. The effects of $\rho(p,T)$ and $\mu(T)$ variation on convective-flow are indirect and lead to: (i) induce radial velocity which alters $u(r)$ profile significantly and (ii) change in $(\partial u/\partial r)_w$ along the flow. It is proposed that the deviation in convection with $C_p(T)$, $k(T)$ variation is significant through temperature field than $\rho(p,T)$, $\mu(T)$ variation on velocity field. It is noted that Nu due to variation in properties differ from invariant properties ($Nu = 48/11$) for low subsonic flow.

1. Introduction

The miniaturised electronic devices are faster, lighter, compact and complex, which often require cooling to avoid overheating. These devices have dimensions in the order of micron and therefore termed as micro-flow devices (MFD). The MFD are having numerous applications in diverse areas viz. cooling of integrated circuit, microelectronic, microfuel cell, microturbine, microscale heat exchanger, microspace craft control, avionics and bioengineering. The miniaturisation technology aggravates the problem of overheating of electronic components and leads to high heat flux dissipation. High performance, high speed MFD requires high rate of heat removal and therefore efficient thermal design and control methods are essential. Over the last decade major attention has been given to MFD due to shrinking dimensions and low coolant requirement. Therefore, it is necessary to understand micro-flow characteristics in transport phenomena which are the focus of present research.

Microchannel heat sinks using liquid as coolant were first proposed for cooling of electronic devices by Tuckerman and Pease [1]. Several researchers [2–5] have carried out theoretical and experimental investigations in microfluidics. They reported deviation in laminar micro-flow characteristics of gas/liquid compared to deviation observed in macro-flow. Sobhan and Garimella [6] presented comparison of studies on fluid flow and heat transfer in micro and minichannels. Their solution partly explains the discrepancies between experimental results and conventional correlations for larger tube. Single-phase micro-convection has been extensively reviewed and summarized by Palm [7] and Rostami et al. [8]. They argued that micro-flow characteristics can not be predicted by conventional theory and classical correlation due to probable reasons of compressibility and rarefaction effect. Steinke and Kandlikar [9] proposed a comparative analysis to focus on departure of flow behaviour in microchannel from conventional channel. They concluded that conventional Stokes and Poiseuille flow theories are applicable in micro-flows. Mahulikar et al. [10] have recently reviewed the literature on microscale fluid flow and reported deviations of heat transfer due to important scaling effects that are significant at microscale. There are deviations in the result of heat transfer characteristics due to various scaling effects, whose significance has been discussed by Morini [11].

In conventional channel, Nu remains constant for laminar forced convection under constant wall heat flux boundary condition (CWHF BC). However, numerical results using continuum approach and experimentally determined Nu for micro-flows have been found to be sometimes agreed [9] and otherwise contradicted with correlations for macro-tubes [12–15]. Mokrani et al. [16] confirms that the continuum mechanics laws for liquid convection remain valid in microchannel for hydraulic diameter (D_h) $\geq$ 100 μm. They observed that Nu for laminar region is in good agreement with well known analytical data presented by Shah and London [17].

* Corresponding author. Tel.: +91 (0)22 25767122; fax: +91 (0)22 25722602.
E-mail address: spm@aero.iitb.ac.in (S.P. Mahulikar).

1290-0729/$ – see front matter © 2009 Elsevier Masson SAS. All rights reserved.
doi:10.1016/j.ijthermalsci.2009.11.001

Nomenclature

D	diameter of micro-tube [m]
h	heat transfer coefficient [W m^{-2} K^{-1}]
L	length of micro-tube [m]
m	mass flow rate [kg s^{-1}]
p_m	cross-sectional average pressure [N m^{-2}]
r, z	radial and axial cylindrical coordinate [m]
$T(r)$	temperature profile in radial direction [-]
T_m	bulk mean temperature [K]
T_0	inlet temperature [K]
T_w	temperature of wall [K]
$u(r)$	axial velocity profile in radial direction [-]
$v(r)$	radial velocity profile in radial direction [-]
q''_w	heat flux at wall [W m^{-2}]
$(\partial u/\partial r)_w$	wall velocity gradient [s^{-1}]
$\partial T/\partial r$	radial temperature gradient [K m^{-1}]
$\partial T_m/\partial z$	bulk mean axial temperature gradient [K m^{-1}]

Greek symbols

γ	specific heat ratio [-]
$\Re$	universal gas constant [= 287 J kg^{-1} K^{-1}]
$\rho(p,T)$	pressure and temperature dependant density [kg m^{-3}]
$C_p(T)$	temperature dependant specific heat at constant pressure [J kg^{-1} K^{-1}]
$k(T)$	temperature dependant thermal conductivity [W m^{-1} K^{-1}]
$\mu(T)$	temperature dependant viscosity [N s m^{-2}]
τ_w	shear stress at wall [N m^{-2}]
$S_{\rho T}$	density temperature sensitivity ($\partial\rho/\partial T$)
$S_{\rho p}$	density pressure sensitivity ($\partial\rho/\partial p$)
S_{Cp}	specific heat temperature sensitivity ($\partial C_p/\partial T$)
S_k	thermal conductivity temperature sensitivity ($\partial k/\partial T$)
S_μ	viscosity temperature sensitivity ($\partial\mu/\partial T$)

Dimensionless numbers

Kn	Knudsen number $\mu_m(\pi)^{0.5}/\rho_m(2\mathscr{R}T_m)^{0.5}$
M	Mach number $u_m/(\gamma\mathscr{R}T_m)^{1/2}$
Nu	Nusselt number hD/k_m
Pe	Peclet number $\rho_m u_m C_{pm} D/k_m$
Re	Reynold number $\rho_m u_m D/\mu_m$

Subscripts

CP	constant properties
D	based on diameter
in	value at inlet
ex	value at outlet
m	mean value, properties evaluated at bulk mean temperature, T_m
w	condition at wall

In a recent study by Lee et al. [12], it is pointed out that discrepancy between numerical results based on conventional approach and experimental data is due to mismatch of (i) boundary conditions (BCs) and (ii) geometry selected for comparison.

Over the last decade, the literature on micro-flow shows inconsistencies between experimental results and correlations. The deviation is due to following reasons: (i) geometric configuration, (ii) uncertainties in measurement of dimensions, (iii) measurement errors in fluid and surface temperatures, (iv) variations in fluid properties, (v) nature of thermal and flow boundary conditions and (vi) conjugate heat transfer between wall and fluid. It is observed that the correlations for macrochannels are not applicable at the microscale and the results are deviated [11,18–20]. To explain these deviations modifications to the BCs are given by scaling effects. For gas flows, the scaling effect is classified into rarefaction and non-rarefaction. The rarefaction scaling effects arises because of failure of continuum assumption, while non-rarefaction effects are those effects which do not require modification of Navier–Stokes equation. Thus, it includes terms which are prominent at the microscale and often neglected in conventional channel analysis. The important scaling effects at microscale are axial conduction, viscous dissipation, compressibility effect and property variation due to steep gradients. The property variation is one of the non-rarefaction effects that increasingly play a vital role from macro-to-microscale convection and this paper focuses on its role in micro-convection performance.

1.1. Literature review on variations in fluid properties

The MFD are characterized by low Re and high q''_w. The variations of fluid properties in micro-convection are much stronger due to steeper temperature gradients and hence its role is significant. As dimensions of these devices reduce, the temperature dependent properties predominantly influence the heat transfer, friction factor and flow profile. It has been also observed that effect of $\mu(T)$ is non-negligible in simultaneously developing laminar flow at low Re [21,22]. Li et al. [23] numerically studied the effect of variation in thermophysical properties with temperature at low Re. They observed that both average and variable properties methods results in high h and lower friction coefficient than theoretical prediction. Further, they confirmed that variable property method is accurate in predicting Nu than inlet property and average property methods. Toh et al. [24] observed that the heat input lowers the frictional losses particularly at low Re regime. They reported that increase in temperature of fluid leads to decrease in $\mu(T)$ and found that $k(T)$ variation has negligible effect on friction factor.

Previously, Bradley and Entwistle [25] have studied effect of property variation for fully-developed flow in a circular tube. They presented a numerical solution at constant wall temperature for air in the range 350–2500 K and noted that fluid acceleration makes substantial axial momentum change. Earlier, reference temperature method and property ratio-method [17,26] were used for correcting Nu in conventional channel which fails to predict convection for large q''_w. Further, Herwig [27] studied the effect of variable properties by asymptotic method (AT) using linear temperature dependence of fluid properties. In AT, axial conduction term in energy equation $[\partial/\partial z(k\cdot\partial T/\partial z)]$ along the flow direction was not considered since it assumes small q''_w. In above methods r-momentum equation was not solved, since it was assumed that Re is high. This theory was precise and unable to provide convection at large q''_w. In a nutshell, AT is suitable only for conventionally sized channel where Re is large and q''_w is small.

In line with above investigation, Mahulikar and Herwig [28] theoretically demonstrated the increasing significance of $\mu(T)$ and $k(T)$ from macro-to-microscale convection. Later, distortion of $u(r)$ profile due to $\mu(T)$ and axial conduction due to $k(T)$ variation was numerically illustrated by Mahulikar and Herwig [29]. They observed that the deviation in liquid convection due to $k(T)$ exceeds the deviation due to $\mu(T)$ variation. The Nu can be changed by 70% due to net effect of induced radial, modified axial

convection and $\rho(p,T)$ variation [30]. Further, they computationally demonstrated that the ratio of radial to axial convection tends to be of the order of one [31]. Thus, $r_{cv} = \int_0^R v(\partial T/\partial r)r\cdot dr / \int_0^R u(\partial T/\partial z)r\cdot dr \rightarrow O(1)$, hence, radial convection mechanism can not be ignored at microscale. They found that local *Nu* increases with increase in q''_w due to influence of variations in $\mu(T)$ and $k(T)$. They also observed that laminar gas micro-convection characteristics are significantly affected by physical effects of variations in properties, since, radial flow is induced with $\rho(p,T)$ and $\mu(T)$ variations due to flow continuity [32]. Recently Gulhane and Mahulikar [33] numerically studied the variations in properties for Graetz problem with low subsonic flow. They reported that deviation in *Nu* is due to significant effect of $s_{\rho T}$ which results from steep temperature gradients. The above mentioned investigation uses high q''_w and low *Re*, which is better suited for micro-flows. Thus, it is noticed that attempts have been made to solve *r*-momentum equation which was ignored in property ratio and AT methods [28–33]. At microscale, additional physical mechanisms are required to determine micro-convection characteristics. Therefore, the role of property variation using *r*-momentum equation approach is more important.

1.2. Objective and scope of investigation

The researchers so far did not explore the role of $C_p(T)$ variation without entrance effect in the literature. This aspect motivates researchers to understand fundamental differences in various physical mechanisms induced by $C_p(T)$, $k(T)$ and $\mu(T)$ in conjunction with $\rho(p,T)$ variation. The existence of high temperature gradient in microscale devices implies that associated temperature dependent property gradients are also high. The various mechanisms that influence the *Nu* are: (i) radial convection, (ii) radial conduction, (iii) axial convection and (iv) axial conduction. The present work numerically illustrates the role of property variation in velocity and temperature fields and its contribution to laminar gas micro-convection with high aspect ratio geometry. This is a sequel of the work presented by Mahulikar and Herwig [32], wherein property variation is coupled with fully-developed flow. The main objective of the present work is to investigate role of $\rho(p,T)$, $C_p(T)$, $k(T)$ and $\mu(T)$ in each of the above mentioned four mechanisms and especially the influence of $C_p(T)$ on axial temperature gradient, axial conduction, Conductance number, and Nusselt number.

2. Description of the problem

A circular cross-section with aspect ratio $(L/D) = 100$ is subjected to CWHF BC as shown schematically in Fig. 1. For all investigated cases, the following input data is fixed:

$R = 375 \times 10^{-6}$ m, $L = 75 \times 10^{-3}$ m, $T_{0,in} = 273$ K and $\rho_m u_m = 16.96$ kg/m^{2}s. The effects of variation in properties are computed with $u_{m,in} = 20$ m/s, $q''_w = 5$W/cm^2 and $Re_{in} = 518$. The q''_w values can be much higher and $u_{m,in}$ much lower for smaller micro-tubes. These values are selected on the basis that maximum temperature of air ($T_{w,ex}$) in the computational domain should not exceed its dissociation temperature.

The *L*/*D* value is selected to ensure that (i) highest *Kn* and *M* in domain is less than 0.001 and 0.3, respectively and (ii) the rates of change of dimensionless profiles of transport variables (u, v, T) along the flow are equated to zero. To simulate the problem, computational domain is mapped with structured and refined grids. This ensures high densities in the vicinity of walls and in the inlet region where high gradients exist. A graded mesh is used in order to capture abrupt change in flow and temperature fields in both directions. A mesh comprises of 40 000 cells [= 400 (axial direction) × 100 (radial direction)] with grid successive ratio 1.01 in axial and 0.99 in radial direction.

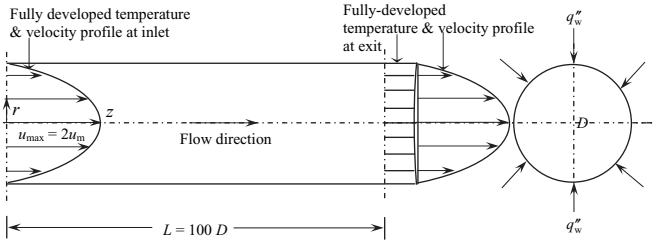

Fig. 1. Schematic of circular tube with constant wall heat flux boundary condition.

2.1. Mathematical modelling of heat transfer

The steady-state, two-dimensional, compressible, continuum-based laminar conservation equations in cylindrical co-ordinates (with axisymmetry) are numerically solved for the above described domain. The equations incorporating ρ, C_p, μ and k variation for convective-flow in uniform cross-section in dimensional and non-dimensional forms are as follows.

2.1.1. Conservation equations

2.1.1.1. Continuity equation

2.1.1.1.1. Dimensional form

$$v\cdot(\partial\rho/\partial r)+\rho\cdot(\partial v/\partial r)+(\rho\cdot v/r)+\rho\cdot(\partial u/\partial z)+u\cdot(\partial\rho/\partial z)=0; \quad (2.1)$$

2.1.1.1.2. Non-dimensional form

$$(\bar{S}_{\rho T}\cdot\Pi_{S\rho T,in})\cdot[\bar{v}\cdot(\partial\theta/\partial\bar{r})+(\bar{u}/2)\cdot(\partial\theta/\partial\bar{z})]+(\bar{\rho}\cdot\bar{v}/\bar{r}) +\bar{\rho}\cdot(\partial\bar{v}/\partial\bar{r})+(\bar{\rho}/2)\cdot(\partial\bar{u}/\partial\bar{z}) = 0; \quad (2.1.1)$$

2.1.1.2. Z-momentum equation

2.1.1.2.1. Dimensional form

$$\rho\cdot[v\cdot(\partial u/\partial r)+u\cdot(\partial u/\partial z)] = -(\partial p/\partial z)+[(\mu/r)+(\partial\mu/\partial r)]\cdot(\partial u/\partial r)+\mu\cdot[(\partial^2u/\partial r^2)+(\partial^2u/\partial z^2)]+(\partial\mu/\partial z)\cdot(\partial u/\partial z); \quad (2.2)$$

2.1.1.2.2. Non-dimensional form

$$\bar{\rho}\cdot Re_{D,in}\cdot[2\bar{v}\cdot(\partial\bar{u}/\partial\bar{r})+\bar{u}\cdot(\partial\bar{u}/\partial\bar{z})] = -(\partial\bar{p}/\partial\bar{z})+(\bar{S}_\mu\cdot\Pi_{S\mu,in})\cdot[4(\partial\theta/\partial\bar{r})\cdot(\partial\bar{u}/\partial\bar{r})+(\partial\theta/\partial\bar{z})\cdot(\partial\bar{u}/\partial\bar{z})]+\bar{\mu}\cdot[4(\partial\bar{u}/\partial\bar{r})/\bar{r}+4(\partial^2\bar{u}/\partial\bar{r}^2)+(\partial^2\bar{u}/\partial\bar{z}^2)]; \quad (2.2.1)$$

2.1.1.3. r-Momentum equation

2.1.1.3.1. Dimensional form

$$\rho\cdot[v\cdot(\partial v/\partial r)+u\cdot(\partial v/\partial z)] = -(\partial p/\partial r)+[(\partial\mu/\partial r)-(\mu/r)]\cdot(v/r)+[(\partial u/\partial r)+(\mu/r)]\cdot(\partial v/\partial r)+\mu\cdot[(\partial^2v/\partial r^2)+(\partial^2v/\partial z^2)]+(\partial\mu/\partial z)\cdot(\partial v/\partial z); \quad (2.3)$$

2.1.1.3.2. Non-dimensional form

$$\begin{aligned}\overline{\rho}\cdot Re_{D,in}\cdot[2\overline{v}\cdot(\partial\overline{v}/\partial\overline{r})+\overline{u}\cdot(\partial\overline{v}/\partial\overline{z})] &= -2(\partial\overline{p}/\partial\overline{r})+(\overline{S}_{\mu}\cdot\Pi_{S\mu,in})\\ &\cdot\{4(\partial\theta/\partial\overline{r})\cdot[(\overline{v}/\overline{r})+(\partial\overline{v}/\partial\overline{r})]\\ &+(\partial\theta/\partial\overline{z})\cdot(\partial\overline{v}/\partial\overline{z})\}\\ &+\overline{\mu}\cdot\{4[(\partial\overline{v}/\partial\overline{r})/\overline{r}\\ &+(\partial^2\overline{v}/\partial\overline{r}^2)-(\overline{v}/\overline{r}^2)]\\ &+(\partial^2\overline{v}/\partial\overline{z}^2)\}; \qquad (2.3.1)\end{aligned}$$

2.1.1.4. Energy equation

2.1.1.4.1. Dimensional form

$$\begin{aligned}\rho\cdot C_p\cdot[v\cdot(\partial T/\partial r)+u\cdot(\partial T/\partial z)] &= [(k/r)+(\partial k/\partial r)]\cdot(\partial T/\partial r)\\ &+k\cdot(\partial^2T/\partial r^2)\\ &+(\partial k/\partial z)\cdot(\partial T/\partial z)\\ &+k\cdot(\partial^2T/\partial z^2)+\mu\cdot\{[(\partial v/\partial z)\\ &+(\partial u/\partial r)]^2+(4/3)[(\partial v/\partial r)^2\\ &+(v/r)^2+(\partial u/\partial z)^2-(\partial v/\partial r)\\ &\cdot(v/r)-(\partial v/\partial r)\cdot(\partial u/dz)\\ &-(v/r)\cdot(\partial u/\partial z)]\}; \qquad (2.4)\end{aligned}$$

2.1.1.4.2. Non-dimensional form

$$\begin{aligned}\overline{\rho}\cdot\overline{C}_p\cdot Pe_{D,in}\cdot[2\overline{v}\cdot(\partial\theta/\partial\overline{r})+\overline{u}\cdot(\partial\theta/\partial\overline{z})] &= (\overline{S}_k\cdot\Pi_{Sk,in})\cdot[4(\partial\theta/\partial\overline{r})^2\\ &+(\partial\theta/\partial\overline{z})^2]\\ &+\overline{k}\cdot[4(\partial\theta/\partial\overline{r})/\overline{r}\\ &+4(\partial^2\theta/\partial\overline{r}^2)\\ &+(\partial^2\theta/\partial\overline{z}^2)]\\ &+(Br_{qw})\\ &\cdot[\{(\partial\overline{v}/\partial\overline{z})+2(\partial\overline{u}/\partial\overline{r})\}^2\\ &+16/3\{(\partial\overline{v}/\partial\overline{r})^2\\ &+(\overline{v}/\overline{r})^2+(1/2\partial\overline{u}/\partial\overline{z})^2\\ &-(\partial\overline{v}/\partial\overline{r})\cdot(\overline{v}/\overline{r})\\ &-1/2(\partial\overline{v}/\partial\overline{r})\\ &\cdot(\partial\overline{u}/\partial\overline{z})-1/2(\overline{v}/\overline{r})\\ &\cdot(\partial\overline{u}/\partial\overline{z})\}]; \qquad (2.4.1)\end{aligned}$$

2.1.2. Defining flow parameters

The u and v are the velocities in z (axial) and r (radial) direction. The cross-sectionally averaged, axial velocity and bulk mean temperature are defined as: $u_m = (1/\rho A)\int_A \rho\cdot u(r)\cdot dA$ and $T_m = (1/u_m A)\int_A u(r)\cdot T(r)\cdot dA$, respectively. The non-dimensional temperature and static pressure are given as: $\theta = k_{m,in}(T_{in}-T_{m,in})/q''_w\cdot D$ and $\overline{p} = p\cdot D/\mu_{m,in}\cdot u_{m,in}$ respectively where, subscript 'm' refers to the mean value of the parameter. The other non-dimensional parameters involved in problem formulation are given in Table 1. The $Re_{D,in}$ and $Pe_{D,in}$ are the inlet Reynold and Peclet numbers, respectively. The Brinkman number ($Br_{qw} = \mu_m\cdot u_m^2/q''_w\cdot D$) is based on the ratio of momentum transfer to heat transfer from the wall and its value reduces with high q''_w and low u_m and vice-versa. The other parameters in equations (2.1)–(2.4) are as follows: $\Pi_{S\rho T,in} = S_{\rho Tm,in}\cdot q''_w\cdot D/(\rho_{m,in}\cdot k_{m,in})$, $\Pi_{S\mu,in} = S_{\mu m,in}\cdot q''_w\cdot D/(\mu_{m,in}\cdot k_{m,in})$, $\Pi_{Sk,in} = S_{km,in}\cdot q''_w\cdot D/k^2_{m,in}$.

In Energy Eq. (2.4), Br_{qw} is a multiplier to viscous dissipation term while its reciprocal appears as multiplier to temperature term. High q''_w and low u_m yield small Br_{qw} which indicate strong influence of properties variations on heat transfer characteristics. The $\Pi_{S\mu,in}$ shows importance of momentum transport over energy transport due to $\mu(T)$ variation whereas, $\Pi_{Sk,in}$ shows relative importance of momentum transport due to $k(T)$ variation and the energy flow due to fluid conduction. Therefore, higher value of these (Π) parameters indicate predominant influence due to variations in properties.

2.1.2.1. Basic equations used in the simulation. The Nu ($= h\cdot D/k_m$) is dimensionless temperature gradient at the surface which can be defined as heat convected axially to heat conducted radially and for CWHF BC it can be written as:

$$Nu = q''_w\cdot D/(T_w - T_m)\cdot k_m \qquad (2.5)$$

The k_m is average over the cross-section and T_m is enthalpy-average temperature of the bulk and

$$T_m = \int_0^R \rho(r)\cdot u(r)\cdot C_p(r)T(r)r\,dr \Big/ \int_0^R \rho(r)\cdot u(r)\cdot C_p(r)r\,dr \qquad (2.5.1)$$

The $T_{m,in}$ can be obtained from above Eq. (2.5.1) using $u_{in}(r)$ and $T_{in}(r)$ profile, as:

$$T_{m,in} = T_{0,in} + (7/24)\cdot[q''_w\cdot R/k(T_{m,in})] \qquad (2.5.2)$$

where, k is iteratively evaluated at $T_{m,in}$ by Netwon-Raphson method.

2.1.3. Boundary conditions

The governing equations (2.1)–(2.4) are numerically solved using following four thermal and flow BCs.

(1) *Inlet*: At the inlet-upstream ($z = 0^-$) fully-developed $u(r)$ and $T(r)$ profiles are respectively given as, $u_{in}(r) = 2u_{m,in}\cdot(1-\overline{r}^2)$ and $T_{in}(r) = T_{0,in} + (q''_w\cdot R/k)\cdot[\overline{r}^2 - (\overline{r}^4/4)]$ [34]. The $T_{0,in}$ is the inlet gas temperature at the axis of micro-tube and $u_{m,in}$ is inlet mean axial velocity. The constant mass flow rate is evaluated as: $m = \rho_m(\pi/4D^2)u_m$ and $\partial u/\partial z = 0$, $v_{in} = 0$.

(2) *Outlet*: At the exit ($z = L$), static pressure is assumed to be constant; specified as $p_{exit} = p_{atm} = 1.01325\times10^5$ Pa. Neumann BCs are imposed on transported variables (u,v,T). The axial temperature gradient is specified based on integral enthalpy balance as: $(dT/dz)_{ex} = 4q''_w/[(\rho\cdot u)_m\cdot D\cdot C_{pm,ex}]$ and $v_{ex} = 0$.

Table 1
Dimensional and non-dimensional variable.

1	C_p	k	μ	ρ	z	u
2	$\overline{C}_p = C_p/C_{pm}$	$\overline{k} = k/k_m$	$\overline{\mu} = \mu/\mu_m$	$\overline{\rho} = \rho/\rho_m$	$\overline{z} = z/D$	$\overline{\mu} = \mu/\mu_m$
3	S_{Cp}	S_k	S_μ	$S_{\rho T}$	$S_{\rho P}$	v
4	$\overline{S}_{Cp} = S_{Cp}/S_{Cpm}$	$\overline{S}_k = S_k/S_{km}$	$\overline{S}_\mu = S_\mu/S_{\mu m}$	$\overline{S}_{\rho T} = S_{\rho T}/S_{\rho Tm}$	$\overline{S}_{\rho p} = S_{\rho p}/S_{\rho pm}$	$\overline{v} = v/\mu_m$

Note: Variables in row 1 & 3 are dimensional while, variables in row 2 & 4 are non-dimensional.

(3) *Wall*: At the wall ($r = R$), $u_w = 0$ (no u-slip) and $v_w = 0$ are applied at non-porous and rigid wall and for CWHF BC 'q''_w = const.', $(\partial T/\partial r)_w = q''_w/k_w$.
(4) *Axis*: At the axis ($r = 0$), symmetric BCs are applied, hence, $(\partial u/\partial r) = (\partial T/\partial r) = (\partial p/\partial r) = (\partial \rho/\partial r) = 0$ and $v = 0$.

From inlet-downstream upto exit ($z = 0^+$ to $z = L$) $\rho(p,T)$, $C_p(T)$, $\mu(T)$ and $k(T)$ variations are modelled. Inlet BC reveals the role of property variation without mixing with entrance effects and gas convective-flow is considered as Newtonian, single-phase, viscid and non-isothermal.

2.2. Solution methodology

The above mentioned governing equations along with ideal gas equation ($p = \rho \cdot \mathscr{R} \cdot T$) are solved with proper relationship using *segregated implicit*, finite volume differencing scheme. This determines five unknown field variables (ρ, u, v, p, T), which provides fluid flow characteristics and energy transfer in a moving fluid. In order to discretize the convective terms in the momentum and energy equations, second order upwind advection scheme is used. For pressure correction simple algorithm is used to secure good convergence and the residual for flow variable is monitored to check the convergence. The convergence criterion is fixed such that plots of residuals for energy, z and r momentum and continuity equations are less than 10^{-12} and these residuals are independent of number of iterations.

2.3. Validation

The accuracy of numerical results is ensured by validating Nu_D results with constant property solution due to CWHF BC [17]. The results are confirmed with benchmarked solution ($Nu_{CP} = 4.36$) and shows a relative error lower than 0.04%. Grid independence tests were performed for grid aspect ratio ($\Delta z/\Delta r) = 50$ and the maximum deviations in Nu_D for the following grids are yield within 0.12%: 400×100 [$(\Delta z/\Delta r) = 50$], 600×150 [$(\Delta z/\Delta r) = 50$], 400×200 [$(\Delta z/\Delta r) = 100$] and 400×50 [$(\Delta z/\Delta r) = 25$]. The enthalpy balance error is calculated for all cases of property variations and maximum error between inlet and exit enthalpy is found to be less than 0.08% ($\delta H_{max} < 0.08\%$). The $T_{m,in}$ values are validated by analytical solutions for cases of all properties constant and $\rho(p,T)$ variation only, and maximum deviation is observed within 0.1%.

The global aspect ratio ($L/D = 100$) is chosen large enough based on: (i) fully-developed profile at exit and it is reasonable to post $\partial/\partial z = 0$ as BC at $z = L$, (ii) need to capture the physical mechanism, (iii) complexity of domain, and (iv) computational cost and time. The highest Kn in the computational domain is lower by one order of magnitude from, 0.001. This ensures that for the solution of continuum-based governing equations Eqs. (2.1)–(2.4), the no-velocity-slip and no-temperature-jump BC at the wall are valid.

3. Results and discussions

The average value of C_p (= 1018.2 J/kg-K) is used for the operating temperature range of 273–550 K, since, the deviation from average value is less than 3%. For the range of 550–2100 K, $C_p(T)$-variation is obtained by least-square error fourth-order polynomial fit within accuracy of 0.12% in following form [35].

$C_p(T) = 874.687 + 0.325431\,T + -2.07132 \times 10^{-5}\,T^2 + -6.63386 \times 10^{-8}\,T^3 + 2.66353 \times 10^{-11}\,T^4$.

For non-reacting and perfect gas: air, $\mu(T) = 1.462 \times 10^{-6} T^{1.5}/(T + 112)$ kg/m·s and $k(T) = 1.9942 \times 10^{-3} T^{1.5}/(T + 112)$, where, T is in K [36].

The results based on velocity and temperature field characteristics are explained in following sections. The effects of property variations are summarized in Table 2 which provides indirect effect on velocity profile due to variation in $\rho(p,T)$ and $\mu(T)$. The direct effect are the effect on fluid temperature field due to variation in $C_p(T)$ and $k(T)$.

3.1. Effect of property variations on velocity field

The effects on velocity field characteristics due to variation in properties are noted as below:

(1) In a micro-tube, heat is conducted radially and acquired thermal energy is carried away through axial convection. Fully-developed flow undergoes a flow development in the vicinity of inlet due to steep temperature gradient [37].

Fig. 2 illustrates $v_m [= (2/R^2) \int_0^R v(r) \cdot r \cdot dr]$ variation along the flow, (a) considering combination of $\rho(p,T)$, $C_p(T)$, $\mu(T)$, $k(T)$ variation, (b) with different q''_w, and (c) different $u_{m,in}$.

(2) The effect of variation in properties induces radial convection while, radial flow and radial velocity (v_m) is induced due to continuity. The v_m is radially outward, (i.e. positive towards increasing radius) reaches to maximum close to inlet and then decays along the flow (Fig. 2).
(3) The variation of v_m versus z/D is shown in Fig. 2(a) for four different cases: (i) $\rho(p,T)$, (ii) $\rho(p,T)$ and $C_p(T)$, (iii) $\rho(p,T)$, $C_p(T)$ and $k(T)$, (iv) $\rho(p,T)$, $C_p(T)$, $k(T)$ and $\mu(T)$. It is seen that radially outward v_m reaches to maximum for the case (i) and (iii) because of dominating effect of $\rho(p,T)$ independently and combined with $k(T)$ variation. The effect of $\rho(p,T)$ is to flatten $u(r)$ profile which promotes faster moving particles near the wall; this enhances the convection. In addition to this, it develops radially outward $v(r)$ which increases conduction thermal resistance in the fluid, thereby degrading the convection.

Table 2
Effects of $\rho(p,T)$, $C_p(T)$, $\mu(T)$ and $k(T)$ variations on micro-convection.

(a) Indirect effect [through velocity (u,v) profiles]

Case	$\rho(r)$: $u(r,z)$	$\rho(r,z)$: $v(r,z)$	$C_p(r)$: $u(r,z)$
$q''_W > 0$(air heated)	Flattens along flow: $Nu \uparrow$	$v(r,z) > 0$ (radially outward): $Nu \downarrow$	Sharpens along flow: $Nu \downarrow$ (insignificant)
Case	$C_p(r,z)$: $v(r,z)$	$\mu(r)$: $u(r,z)$	$\mu(r,z)$: $v(r,z)$
$q''_W > 0$(air heated)	$v(r,z) < 0$ (radially inward): $Nu \uparrow$ (insignificant)	Sharpens along flow: $Nu \downarrow$	$v(r,z) < 0$ (radially inward): $Nu \uparrow$

(b) Direct effect [through fluid temperature field]

Case	$\rho(r)$	$C_p(r)$	$C_{pm}(z)$	$k(r)$	$k_m(z)$
$q''_W > 0$(air heated)	Inverted-U'- shaped: $Nu \downarrow$ (significant)	'U'-shaped: $Nu \uparrow$ (insignificant)	Increasing along flow: $Nu \uparrow$ (significant)	'U'-shaped: $Nu \uparrow$ (significant)	Increasing along flow: $Nu \uparrow$ (significant)

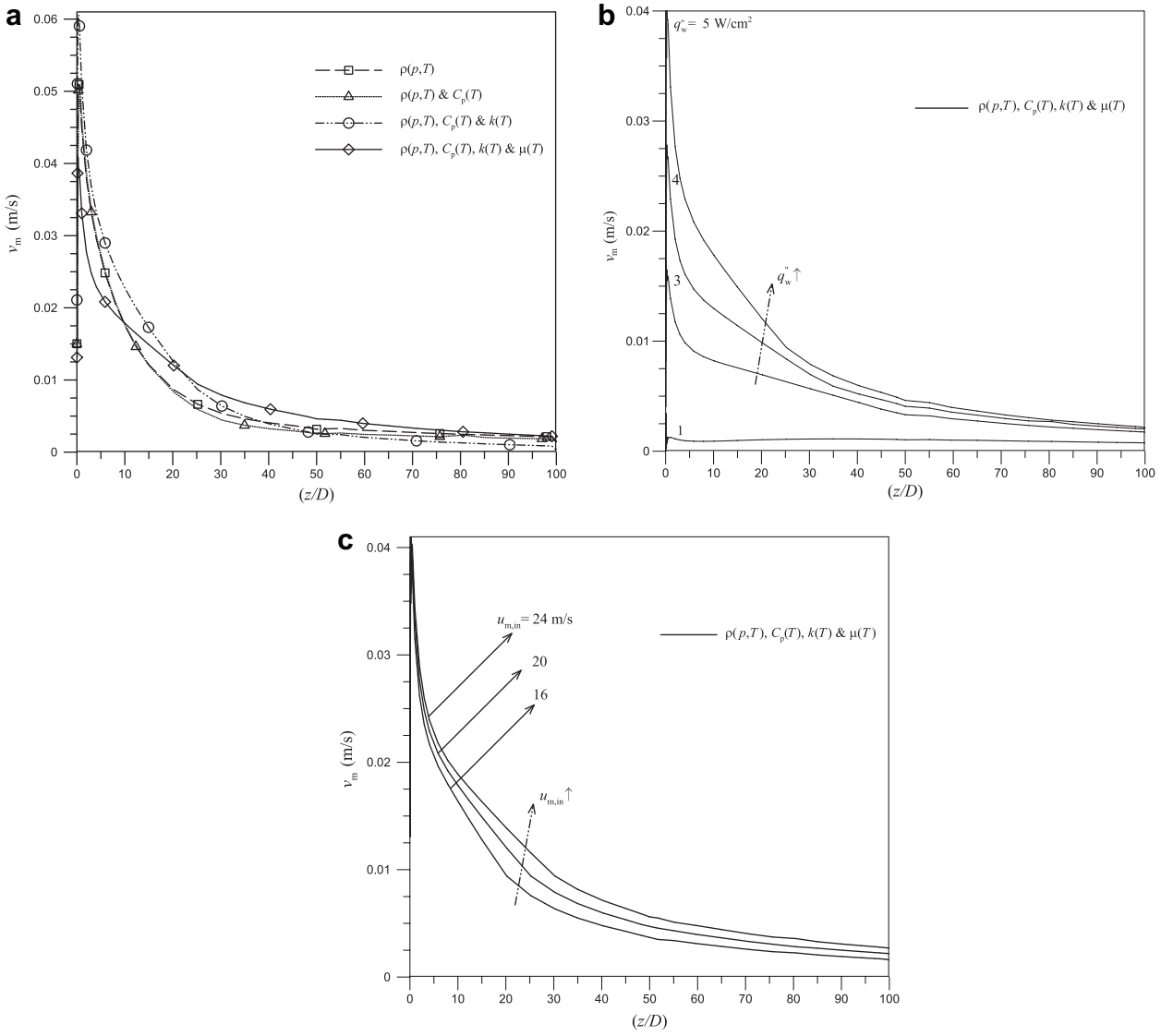

Fig. 2. Variation of v_m along the flow, (a) due to combination of variation in $\rho(p,T)$, $C_p(T)$, $\mu(T)$ and $k(T)$, (b) due to $\rho(p,T)$, $C_p(T)$, $\mu(T)$ and $k(T)$ variation for $u_{m,in} = 20$ m/s and different q''_w, (c) due to $\rho(p,T)$, $C_p(T)$, $\mu(T)$ and $k(T)$ variation for $q''_w = 5W/cm^2$ and different $u_{m,in}$.

(4) For the case of heated air, the effect of $C_p(T)$ and $\mu(T)$ variation is to sharpen $u(r)$ by inducing radially inward $v(r)$ profile. The v_m is radially inward (i.e. negative towards decreasing radius) and in the direction of diffusion of heat which promotes convection. But sharpening of $u(r)$ profile lowers axial mass flux near the wall, thereby retarding convection.

(5) Thus, the effects due to $\rho(p,T)$ and $\mu(T)$ variation in inducing radial flow are opposite to each other and the following trend of v_m is summarized: $v_{m\_(iii)} > v_{m\_(i)} > v_{m\_(ii)} > v_{m\_(iv)}$.

(6) It is seen from Fig. 2(b) and (c) that, increase in the value of q''_w and $u_{m,in}$ increases v_m. This is attributed to: (i) change in ρ gradients along the flow and (ii) increase in v_m with $u_{m,in}$ to conserve the mass. The enthalpy-average temperature of the bulk remains unchanged with different $u_{m,in}$ but not with different q''_w Eq. (2.5.2).

Fig. 3 illustrates $u(r,z)$ profile due to combination of $\rho(p,T)$, $C_p(T)$, $k(T)$ and $\mu(T)$ variation. The parabolic curve for fully-developed constant properties flow is shown for comparison [35]. Due to incorporation of $\rho(p,T)$ variation, the profile changes from parabolic (developed) to most flattened profile (undeveloped mode). Increase in $\rho(p,T)$ variation due to higher q''_w causes more flattening effect which reduces axial velocity at the center. This leads to large mass flux close to wall, thereby promoting convection (since, $Nu \propto (\partial u/\partial r)_w$). Fig. 3 indicates solid line showing re-sharpening and developing profile due to combined effect of $\rho(p,T)$, $C_p(T)$, $k(T)$ and $\mu(T)$. The reasons behind flattening and sharpening effect of $u(r,z)$ profile are mentioned as below:

(i) incorporation of $\rho(p,T)$ and $k(T)$ flattens $u(r)$ profile due to changing velocity and varying density over a heated length of flow and (ii) incorporation of $\mu(T)$ and $C_p(T)$ variation sharpens $u(r)$ profile by inducing inward radial flow.

For micro-tube flow, $\rho(p,T)$ causes axial acceleration which lead to change $u(r)$ profile much flatter than parabolic [18,38]. This alters shape and magnitude of velocity profile that produces additional non-linear pressure drop as the fluid flows downstream [15]. The physical effect of $C_p(T)$ and $k(T)$ variation on axial velocity profile is relatively insignificant.

Fig. 4 illustrates ρ gradients over the cross-section due to combination of $\rho(p,T)$, $C_p(T)$, $k(T)$ and $\mu(T)$ variation. In case of

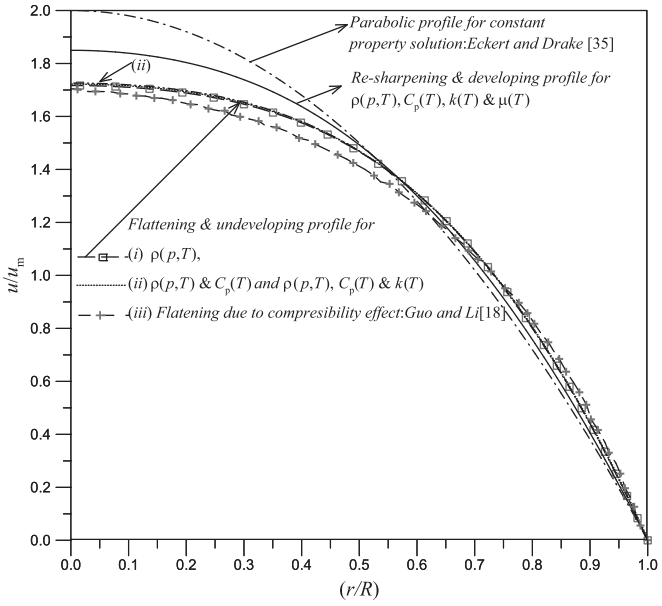

Fig. 3. Radial variation of axial velocity at $z/D = 20$.

heated air, $\rho(r)$ profile is an inverted 'U' shape and lower ρ closer to the wall is less effective in heat transport, thereby degrading convection (Table 2). The $\rho(r)$ profile is an inverse of $T(r)$ profile and 'U' shape $\rho(r)$ profile augments convection. Incorporation of $C_p(T)$ and $k(T)$ variation increases C_{pm} and k_m along the flow which reduces T_w and $(\partial T/\partial r)_w$, respectively. This results in higher ρ closer to the wall which is more effective in heat transport, thereby promoting convection.

3.2. Effect of property variations on temperature field

The temperature field characteristics are governed by fluid and wall surface temperatures, axial conduction and radial conduction. The investigated heat transfer performance essentially shows temperature field characteristics which are described here. Fig. 5 shows variation of T_w and T_m along the flow; T_w is lower due to variation in properties than T_w in constant property flow. The wall temperature monotonically increases along heated flow due to τ_w and friction at wall surface. The maximum temperature of air shall be lower than its dissociation temperature ($T_{w,ex} < 2000$ K). Incorporation of $C_p(T)$ variation increases C_p near the wall which causes reduction in T_w for a given q''_w. Incorporation of $k(T)$ variation increases k_m along the heated flow which reduces T_w due to corresponding temperature gradient (Eq. : $q''_w = k_w \cdot (\partial T/\partial r)_w$). Thus, it is observed that incorporation of $C_p(T)$ and $k(T)$ significantly reduces T_w compared to $\rho(p,T)$ variation alone.

Fig. 5 also shows increasing T_m along the flow because of heat addition to the fluid. The T_m represents total energy of the flow at a particular location in micro-tube and is given by Eq. (2.5.1). The $T_{m,in}$ reduces from 437.4 K to 416.5 K due to incorporation of variation in properties. The rate of change of T_m is lower for the case of $C_p(T)$ variation only, than for other cases of property variation. This is due to increase in $C_p(T)$ that reduces u_m (as $u_m \propto T_m/p_m$). Therefore, it noticed that the effect of $C_p(T)$ variation is significant in temperature field than velocity field.

Fig. 6 shows rate of change of T_w along the flow; $(\partial T_w/\partial z > 0)$ is not constant for various cases of property variation unlike constant property solution. Initially $(\partial T_w/\partial z)$ goes to the maximum due to higher τ_w; reduces slightly and further increases non-linearly except for $\rho(p,T)$ and $C_p(T)$ variation. This can be attributed to: (i) incorporation of $\rho(p,T)$ variation causes flattening of $u(r)$ profile which causes increase in $(\partial u/\partial r)_w$, τ_w and T_w (since, $\tau_w = \mu_w \cdot (\partial u/\partial r)_w$) and (ii) higher flattening near the inlet. The decrease in T_w due to $k(T)$ variation is higher than $C_p(T)$ variation, therefore, $(\partial T_w/\partial z)$ reduces along the flow for $\rho(p,T)$ and $C_p(T)$ variation. The values of $(\partial T_w/\partial z)$ are lower for the cases incorporating $k(T)$ variation compared to constant property solution and $(\partial T_w/\partial z)_{\text{without } k \text{ variation}} > (\partial T_w/\partial z)_{\text{with } k \text{ variation}}$.

Fig. 7 illustrates variation of rate of change of T_m along the flow, i.e. $\partial T_m/\partial z$, bulk mean axial fluid temperature gradient. For constant property solution, $\partial T_m/\partial z$ remains unchanged as the fluid flows downstream. It is observed that incorporation of $C_p(T)$ significantly reduces $\partial T_m/\partial z$ compared to $\rho(p,T)$ variation alone. The reasons attributed are (i) axial fluid temperature profile $T_m(z)$ is non-linear for the cases where C_p varies and (ii) increase in $\partial C_{pm}/\partial z$ reduces $(\partial T_m/\partial z)$. As $\partial C_{pm}/\partial z > 0$ the term in energy equation $(\partial^2 T_m/\partial z^2 \neq 0)$ and as $\partial k_m/\partial z > 0$ the term $(\partial k/\partial z \cdot \partial T/\partial z)$ increases $\partial T_m/\partial z$. These two

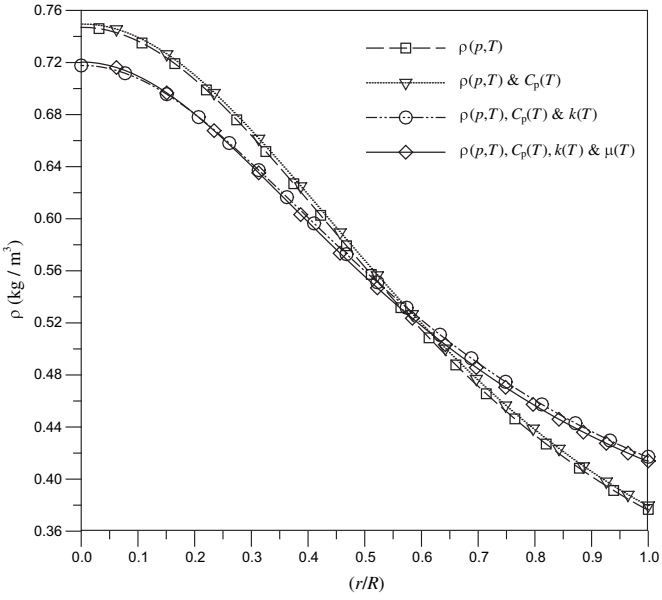

Fig. 4. Radial variation of density at $z/D = 20$.

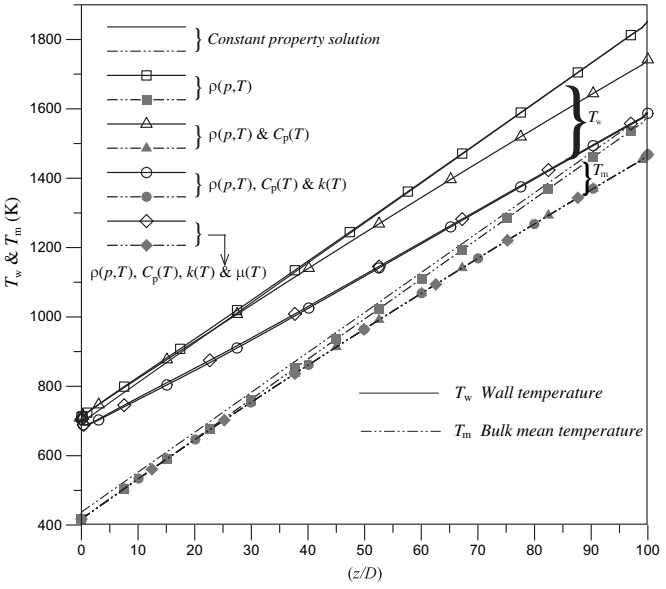

Fig. 5. Variation of T_w and T_m along the flow.

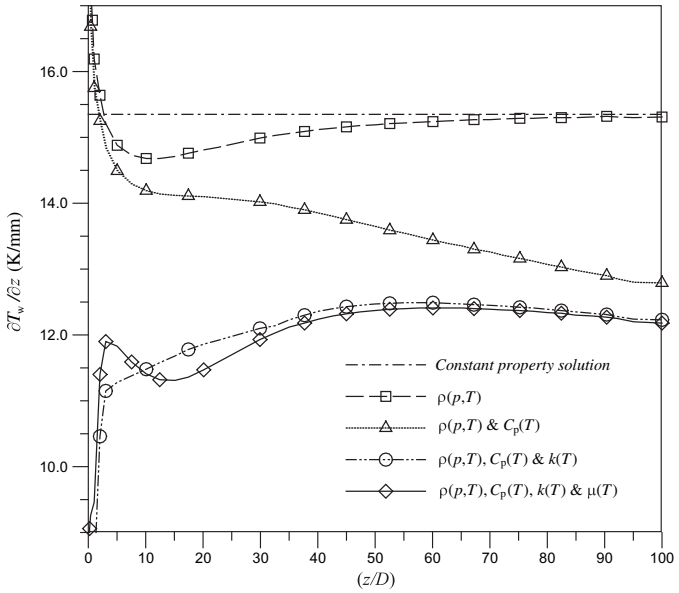

Fig. 6. Variation of $\partial T_w/\partial z$ along the flow.

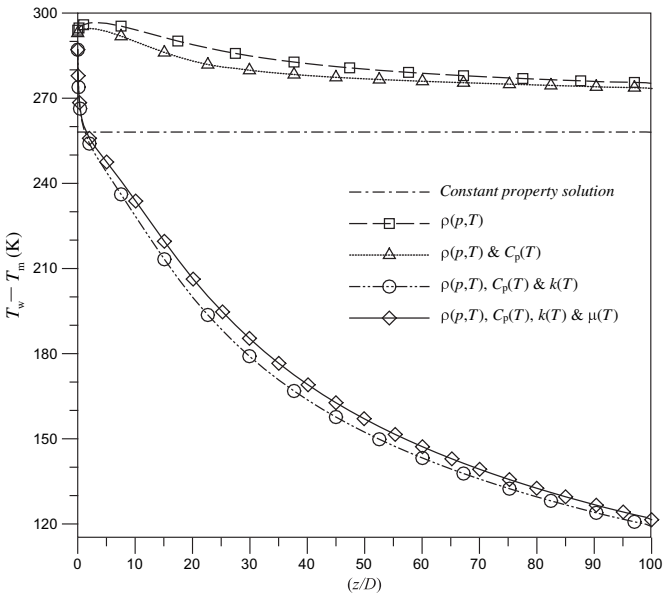

Fig. 8. Variation of $T_w - T_m$ along the flow.

effects lead to develop axial conduction along the flow which shows different heat transfer behaviors compared to conventional channel.

Fig. 8 illustrates $(T_w - T_m)$ along the flow due to "q''_w = const." BC considering variation in properties. The effect of $C_p(T)$ is to reduce T_w and T_m towards the tube exit. The $T_{w,ex}$ and $T_{m,ex}$ reduce by 110 K and 126 K, respectively, while $k(T)$ reduces $T_{w,ex}$ by 263 K irrespective of T_{wCP}. For variation in $C_p(T)$, reduction in T_w causes decrease in T_m and the overall effect is to reduce $(T_w - T_m)$, thereby enhancing *Nu* Eq. (2.5). Increase in C_{pm} along the flow reduces T_w and $(T_w - T_m)$, as $q''_w = m \cdot C_{pm} \cdot (T_w - T_m)$ and increase in k_m along the flow reduces $(\partial T/\partial r)_w$, T_w and $(T_w - T_m)$. Thus, rate of decrease of $(T_w - T_m)$ is higher than constant property solution which is due to dominant role of $k(T)$ and $C_p(T)$ variation. Hence, $C_p(T)$ and $k(T)$ has direct/significant effect through temperature field which enhances convection.

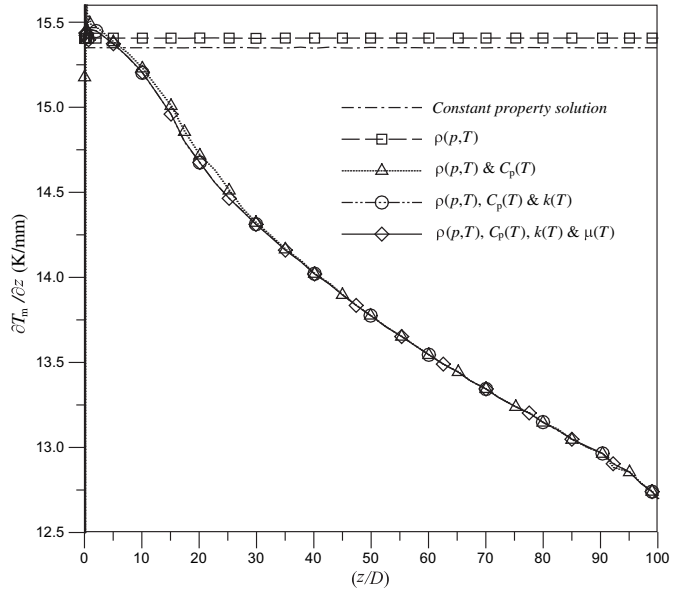

Fig. 7. Variation of $\partial T_m/\partial z$ along the flow.

3.2.1. *Effect of property variations on axial conduction*

Choi et al. [14], Shah and London [17], and Guo and Li [18] studied the effect of axial conduction on h and *Nu*. They observed that decrease in Re and larger conductivity ratio (k_w/k_m) leads to lower *Nu*. Mahulikar and Herwig [29,32] numerically evaluated role of $k(T)$ variation in axial conduction. They found that increase in $\partial k_m/\partial z$ leads to increase axial temperature gradient and *Nu*. The effect of property variation on axial conduction is explained on the basis of axial temperature gradient. The axial conduction term in energy equation is given by $\partial/\partial z(k \cdot \partial T/\partial z) = k \cdot \partial^2 T/\partial z^2 + \partial k/\partial z \cdot \partial T/\partial z$. For $C_p(T)$ variation the term $k \cdot \partial^2 T/\partial z^2$ is non zero, since, axial temperature gradient is not constant and for $k(T)$ variation the term $\partial k/\partial z \cdot \partial T/\partial z$ plays an important role due to $k(z)$ variation.

The effect of $C_p(T)$ variation on axial temperature gradient is obtained based on enthalpy balance along the flow direction as below:

Heat given to fluid element + conduction = Change in internal energy

$$q''_w \cdot \pi D \cdot \Delta z + (\partial k_m/\partial z) \cdot |\partial T_m/\partial z| \cdot \Delta z \cdot (\pi D^2)/4 = \rho_m \cdot [(\pi D^2)/4] \cdot u_m \cdot \partial C_{pm}/\partial z \cdot \Delta z \, \Delta T \quad (3.1)$$

The effect of $C_p(T)$ and $k(T)$ variation on axial temperature gradient is expressed as:

$$|\partial T_m/\partial z| = 4(q''_w/D)/[\rho_m \cdot u_m \cdot (\partial C_{pm}/\partial z) \cdot \Delta z - \partial k_m/\partial z] \quad (3.1.1)$$

Along the axial direction C_{pm} increases as heat addition causes T_m to increase and high $\partial C_{pm}/\partial z$ causes less $|\partial T_m/\partial z|$ Eq. (3.1.1). The role of increasing $\partial C_{pm}/\partial z$ is to reduce axial conduction by reducing $|\partial T_m/\partial z|$. Low value of $|\partial T_m/\partial z|$ reduces *Nu* along the flow, since, lower $|\partial T_m/\partial z|$ indicates lower *Nu* for a given *m*. But *Nu* still increases along the flow because $C_p(T)$ reduces $(T_w - T_m)$ by increasing *h* Eq. (2.5).

The effect of incorporation of $k(T)$ variation is to increase $k_m(z)$ along the flow. The $|\partial T_m/\partial z|$ and *Nu* is higher for $\partial k_m/\partial z > 0$ because, it reduces T_w by increasing *h*. Therefore, $|\partial T_m/\partial z|$ and *Nu* exceeds the case for which $(\partial k_m/\partial z) = 0$ Eq. (3.1.1).

In the present investigation, thickness of wall (Δt) tends to zero, therefore, Biot number $(Bi = h \cdot \Delta t/k_w)$ tends to zero. For thin tube T_w is equal to $T_{f \text{ at } r=R}$, since, q''_w at outer surface and inner surface is same. Therefore, there is no axial conduction in the tube wall.

However, if Δt is assumed to be of the same order as D then the effect of axial heat conduction in wall is given by Conductance number [39]. The Conductance number is ratio between axial heat conduction in tube wall and heat transfer by convection in fluid. Thus, Conductance number $= (k_w \cdot A_w \cdot D)/(k_f \cdot A_f \cdot L \cdot Re \cdot Pr)$, where, k_w, A_w, k_f and A_f are thermal conductivity and cross-sectional area for wall and fluid, respectively. Fig. 9 illustrates variation of Conductance number along the heated flow due to combination of variation in properties. Conductance number for a circular tube is given as: $(k_w \cdot 4D)/\{k_f \cdot Pe \cdot L \cdot [(D/\Delta t) - 1]\}$. In case of conventional tube Δt is very small compared to diameter, hence, Conductance number tends to zero. Therefore, the effect of axial conduction in wall on convective heat transfer is ignored (Conductance number < 0.005). In microscale Δt can be of the same order or larger than D (Conductance number > 0.005), hence, effect of axial conduction in wall can not be ignored.

The *Pe* is measure of thermal energy convected to thermal energy conducted axially within the fluid, the inverse of which indicates the importance of axial conduction in the fluid. The *Pe* increases along the flow for the cases incorporating $C_p(T)$ variation so long as $k(T)$ is not incorporated. Thus, incorporation of $k(T)$ variation reduces *Pe* which increases Conductance number along the flow as $Pe \propto C_{pm}/k_m$. Though the heat transfer in fluid convection is substantial, the axial heat conduction in wall contributes significantly to the net heat transfer.

3.2.2. Effect of property variations on radial conduction

Fig. 10 shows radial temperature profile due to combination of $\rho(p,T)$, $C_p(T)$, $k(T)$ and $\mu(T)$ variations. The temperature of fluid near the wall is higher relative to temperature near the axis of micro-tube due to high q''_w. It is observed from numerical solution that the variation in $C_p(T)$ causes slight alleviation of $(\partial T/\partial r)_w$ which reduces radial conduction and this effect is insignificant. The radial variation of $C_p(T)$ has significant effect on T_m than $(\partial T/\partial r)_w$ and static temperature reduces over the entire r/R by 45 K. The radial variation of $C_p(T)$ plays important role in reducing T_w rather than distorting temperature profile, hence, its role on radial conduction is insignificant.

It has been observed that $k(T)$ variation directly affects the temperature field by flattening the temperature profile. Increase in k_w along the heated flow for constant q''_w reduces $(\partial T/\partial r)_w$, T_w and temperature difference over the cross-section (since, radial heat flow; $q''_w = k_w(\partial T/\partial r)_w$). In case of $k(r)$ variation, higher k fluid near the wall is more effective in convecting away the imposed heat flux at the wall relative to the higher k near the axis of micro-tube. Therefore, effect of $C_p(T)$ and $k(T)$ causes a reduction in T_w for the case of heated air that promotes convection. The effect of $\rho(p,T)$ and $\mu(T)$ on radial conduction is negligible as they do not reduce $(\partial T/\partial r)_w$ considerably.

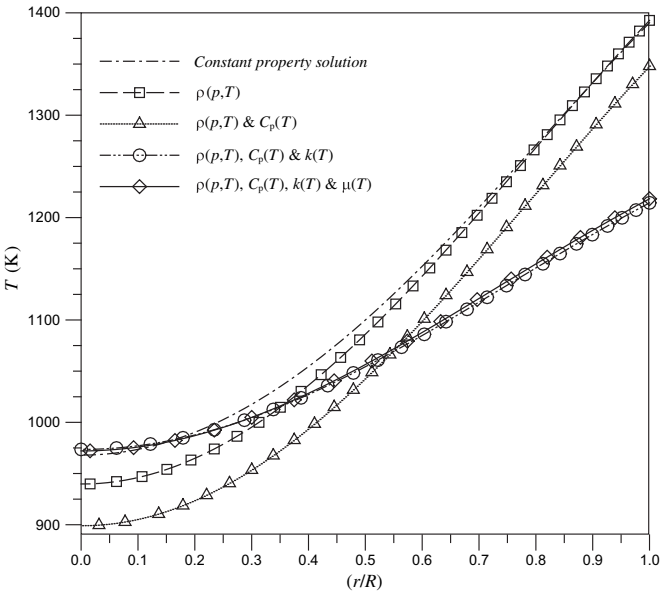

Fig. 10. Radial variation of static temperature.

3.3. Effect of property variations on Nusselt number

Liu et al. [13] numerically studied effect of property variation on local *Nu* with different q''_w and $T_{o,in}$ and observed significant deviation from constant property solution. Fig. 11 illustrates variation in *Nu* along the flow and Table 3 indicates Nu_{min}, $|\Delta Nu_{CP}|/Nu_{exit}$ due to various combination of $\rho(p,T)$, $C_p(T)$, $k(T)$ and $\mu(T)$ variations. The *Nu* is calculated using Eqs. (2.5), (2.5.1) and

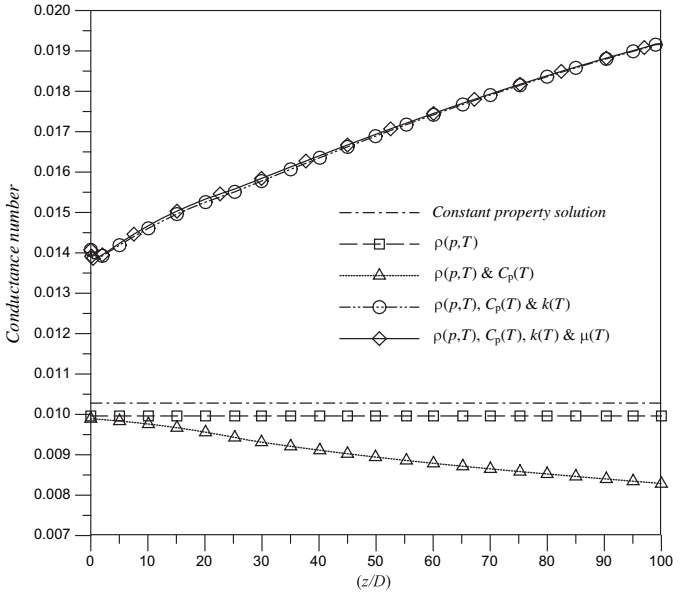

Fig. 9. Variation of Conductance number along the flow.

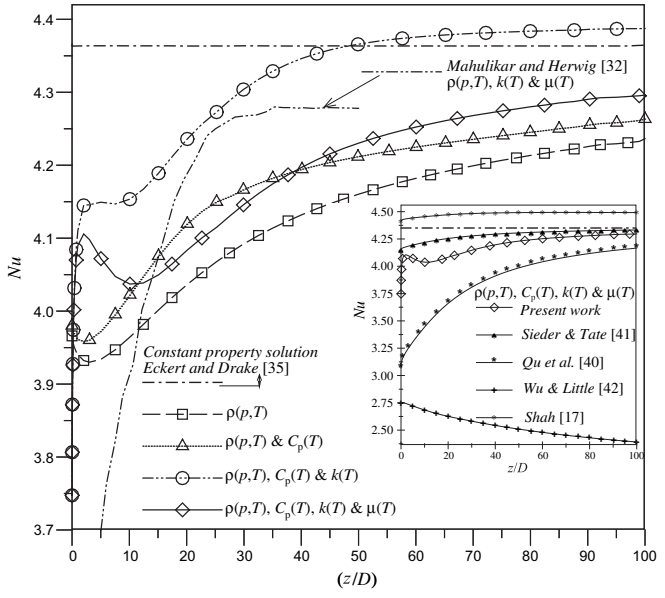

Fig. 11. Variation of *Nu* along the flow.

Table 3
The Nu, $|\Delta Nu_{CP}|$ due to combination of variation in $\rho(p,T)$, $C_p(T)$, $\mu(T)$ and $k(T)$.

Fluid properties combination	Nu_{min}	$\lvert\Delta Nu_{CP}\rvert$ in %	Nu_{exit}	$\lvert\Delta Nu_{CP}\rvert/Nu_{exit}$
Constant property solution	4.36	0	4.36	0
$\rho(p,T)$	3.93	9.86	4.24	2.33
$\rho(p,T)$ and $C_p(T)$	3.96	9.17	4.25	2.16
$\rho(p,T)$, $C_p(T)$ and $k(T)$	3.75	14.01	4.4	3.18
$\rho(p,T)$, $C_p(T)$, $k(T)$ and $\mu(T)$	3.75	14.01	4.31	3.25

$$|\Delta Nu_{CP}| = [(Nu_{min} - Nu_{CP})/Nu_{CP}] \times 100\% \quad (3.2)$$

The comparative study is carried out to note the differences between heat transfer in micro-tube with property variation and that in constant property solution. The simulation result for constant property solution is in good agreement with Eckert and Drake [35]. The Nu in the present study is calculated using CWHF, laminar micro-flow correlation proposed by Sieder and Tate [41], Qu et al. [40], Wu and Little [42] and Shah [17] which is shown in inset of Fig. 11. The Nu due to all property variation reasonably agreed with Sieder and Tate correlation, while deviated from Qu et al. Wu and Little, and Shah correlation. The significant deviations in results are attributed to (i) dimension selected for geometry and (ii) non-rarefaction scaling effect due to variations in properties. The results presented by Mahulikar and Herwig [32] differ from result of present investigation due to different (i) aspect ratio ($L/D = 50$) and (iii) inlet and wall boundary conditions.

Thus, overall heat transfer performance (Nu) is determined jointly by the following features:

(i) Incorporation of $\rho(p,T)$ causes increase in u_m that lead to significant development of v_m. The role of flattening of $u(r)$ profile to change axial convection is more dominant; hence, net Nu increases along the flow. Initial decrease in Nu is because of increase in $(T_w - T_m)$; since, rate of increase of T_m is higher than T_w due to developing flow.
(ii) Incorporation of $C_p(T)$ causes reduction in T_m, which is compensated by decrease in T_w. Therefore, for same q''_w increase in C_{pm} reduces $(T_w - T_m)$ thereby augmenting Nu. The change in axial convection due to $C_p(T)$ exceeds the axial convection due to $\rho(p,T)$ variation which shows the predominant effect of $C_p(T)$ variation on temperature field.
(iii) The rate of increase in Nu is higher for incorporation of $k(T)$ than for $\rho(p,T)$ and $C_p(T)$ variation. The reasons behind this are: (a) increase in k_w reduces $(\partial T/\partial r)_w$, (b) decrease in sharpening of temperature profile and (c) favorable axial conduction, thereby augmenting Nu. The results obtained in present investigation differ from Toh et al. [24], where $k(T)$ variation is found to be insignificant.
(iv) The effect of $\mu(T)$ variation is to sharpen $u(r)$ profile by inducing radially inward $v(r)$ profile. The effect is same as the effect of hydrodynamic development on $u(r,z)$ and $T(r,z)$ profile which degrades Nu marginally. Initial decrease in Nu is due to dominating effect of increase in k_m over decreasing rate of $(T_w - T_m)$.

3.4. Significance of non-dimensional number

Table 4 shows flow properties and non-dimensional number at inlet, exit and $z/D = 50$. A fully-developed flow enters the heated section of the tube and as the heat is absorbed, the temperature of the fluid along the flow starts to increase. In subsonic fluid flow, pressure drops along the length of micro-tube due to acceleration of fluid particle and friction. The density and pressure along the flow reduces and Kn increases. The value of Kn is highest at exit of the tube where, ρ is lowest and exit value of Kn increases with q''_w. This is due to: (i) increase in momentum which contributes to decrease in the pressure and increase in T_m.

The Re decreases towards flow since air viscosity increases with temperature, as the mass flux $(\rho_m \cdot u_m)$ is constant. The M in the problem is much less compared to 0.3; hence, compressibility effects can be neglected [18]. The M increases along the flow for the cases incorporating $\rho(p,T)$ variation and this is due to flow acceleration. But M reduces when $C_p(T)$ variation is incorporated due to lowering of T_m and u_m. For low Mach subsonic flow, gas density variation is due to significant $S_{\rho T}$ resulting from steep temperature gradients and $S_{\rho p}$ is found to be insignificant.

4. Concluding remark

(i) In compressible laminar fluid flow, incorporating different combination of $\rho(p,T)$, $C_p(T)$, $k(T)$ and $\mu(T)$ leads to non-rarefaction scaling effects. It is noticed that Nu deviates significantly from constant property solution; especially in the beginning of the computational domain, though this difference reduces as the flow proceeds.
(ii) The $\rho(p,T)$ variation causes flow acceleration, flattens $u(r)$ profile and increases $(\partial u/\partial r)_w$ along the flow. The net effect of increase in Nu is due to flattening of $u(r)$ profile than outward convection and decreasing effect of ρ variation.
(iii) The reduction in u_m and increase in C_p near wall causes reduction in T_w and $(T_w - T_m)$; although incorporation of $C_p(T)$ reduces $\partial T_m/\partial z$ except $\rho(p,T)$ variation. The net effect is increase in Nu. The effect of $C_p(T)$ is more prominent in high temperature region that helps to reduce wall temperature towards tube exit. The term $\partial^2 T_m/\partial z^2$ in energy equation is non zero which contributes in determining axial conduction in flow.
(iv) The role of $k(T)$ variation is to flatten temperature profile, reduce $(\partial T/\partial r)_w$ and induce favorable axial conduction. The $\partial T_m/\partial z$ induces to occur significant axial conduction along the flow thereby, augmenting Nu.
(v) The effect of $\mu(T)$ variation is to sharpen $u(r)$ profile by inducing radially inward $v(r)$ profile. This leads to non-negligible inward radial convection relative to axial convection which degrades Nu.
(vi) The effect of $\rho(p,T)$ and $\mu(T)$ on convective-flow is indirect and deviation in Nu is significant through velocity field, while deviation in Nu due to $C_p(T)$ and $k(T)$ variation is significant through temperature field.
(vii) The (Π) parameter indicates relative significance of cross flow momentum transport and energy transport due to fluid

Table 4
Flow properties and non-dimensional numbers at different locations of geometry.

Flow properties at →various location and Properties combination ↓	Inlet τ_w,$(\partial\bar{u}/\partial\bar{r})_w$ C_{pm}, k_m 10^3	$z/D = 50$ τ_w,$(\partial\bar{u}/\partial\bar{r})_w$ C_{pm}, k_m 10^3	Exit τ_w,$(\partial\bar{u}/\partial\bar{r})_w$ C_{pm}, k_m 10^3	$Re_{in,exit}$ $M_{in,exit}$ 10^2	$Kn_{in,exit}$ 10^4 $Pe_{in,exit}$
Constant property solution	5.42, 4.02 1019.2, 33.3	5.42, 4.02 1019.2, 33.3	5.42, 4.02 1019.2, 33.3	500, 500 4.8, 2.5	1.41, 0.74 389, 389
$\rho(p,T)$	5.28, 4.02 1015.9, 32.2	14.18, 10.82 1015.9, 32.2	21.45, 16.38 1015.9, 32.2	518, 518 4.9, 9.5	1.41, 2.72 401, 401
$\rho(p,T)$ and $C_p(T)$	5.28, 4.02 1023.1, 32.2	13.64, 10.41 1131.6, 32.2	19.81, 15.12 1221.9, 32.2	518, 518 4.9, 9.2	1.41, 2.62 404, 483
$\rho(p,T)$, $C_p(T)$ and $k(T)$	5.25, 4.02 1023.1, 34.6	13.59, 10.37 1132.3, 56.4	19.76, 15087 1221.9, 71.6	518, 518 4.9, 9.2	1.41, 2.63 373, 217
$\rho(p,T)$, $C_p(T)$, $k(T)$ and $\mu(T)$	7.16, 4.02 1023.1, 34.9	22.75, 9.58 1132.3, 56.5	41.45, 14.28 1221.9, 71.7	518, 235 4.9, 9.2	1.41, 5.8373, 217

conduction. Therefore, high q''_w and low u_m produces higher value of (Π) parameter, which indicates stronger effect due to variations in properties.

Acknowledgments

The authors thank Mr. N.B. Pasalkar, Ex. Director, D.T.E. Mumbai, India and Government Polytechnic, Thane, for extending full support and co-operation. The authors are grateful to the A. von Humboldt Foundation, Germany (grant no. INI/1104249) for the rich exposure to research methodology.

References

[1] D.B. Tuckerman, R.F.W. Pease, High-performance heat sinking for VLSI. IEEE Electron Device Lett. EDL 2 (1981) 126–129.
[2] C.S. Chen, W.J. Kuo, Heat transfer characteristics of gaseous flow in long mini and micro-tubes. Numer. Heat Tran. Part A 46 (2004) 497–514.
[3] W. Owhaib, B. Palm, Experimental investigation of single-phase convective heat transfer in circular microchannels. Exp. Thermal Fluid Sci. 28 (2004) 105–110.
[4] G. Hetsroni, A. Mosyak, E. Pogrebnyak, L.P. Yarin, Fluid flow in microchannels. Int. J. Heat Mass Tranf. 48 (2005) 1982–1998.
[5] Y. Yener, S. Kakaç, M. Avelino, T. Okutucu, Single-phase forced convection in microchannels – state-of-the-art-review. in: S. Kakaç, L. Vasiliev, Y. Bayazitoglu, Y. Yener (Eds.), Microscale Heat Transfer – Fundamentals and Applications in Biological Systems and MEMS. Kluwer Academic Publishers, The Netherlands, 2005.
[6] C.B. Sobhan, S.V. Garimella, A comparative analysis of studies on heat transfer and fluid flow in microchannels. Microscale Thermophys. Eng. 5 (2001) 155–175.
[7] B. Palm, Heat transfer in microchannels. Microscale Thermophys. Eng. 5 (2001) 155–175.
[8] A.A. Rostami, A.S. Mujumdar, N. Saniei, Flow and heat transfer for gas flowing in microchannels: a review. J. Heat Mass Transfer 38 (2002) 359–367.
[9] M.E. Steinke, S.G. Kandlikar, Single-phase liquid friction factors in microchannels. Int. J. Thermal Sci. 45 (2006) 1073–1083.
[10] S.P. Mahulikar, H. Herwig, O. Hausner, Study of gas micro-convection for synthesis of rarefaction and non-rarefaction effects. IEEE/ASME J. MEMS 16 (2007) 1543–1556.
[11] G.L. Morini, Single-phase convective heat transfer in microchannels: a review of experimental results. Int. J. Therm. Sci. 43 (2004) 631–651.
[12] P.S. Lee, S.V. Garimella, D. Liu, Investigation of heat transfer in rectangular microchannels. Int. J. Heat Mass Tranfer 48 (2005) 1688–1704.
[13] J.T. Liu, X.F. Peng, B.X. Wang, Variable-property effect on liquid flow and heat transfer in microchannels. J. Chem. Eng. 141 (2008) 346–353.
[14] S.B. Choi, R.F. Barron, R.O. Warrington, Fluid flow and heat transfer in microtubes in: micromechanical sensors, actuators and systems. ASME DSC 32 (1991) 123–133.
[15] G.P. Celata, M. Cumo, S.J. Mcphail, L. Tesfagabir, G. Zummo, Experimental study on compressible flow in micro-tubes. Int. J. Heat Fluid Flow 28 (2007) 28–36.
[16] O. Mokrani, B. Bourouga, C. Castelain, H. Peerhossaini, Fluid flow and convective heat transfer in flat microchannels. Int. J. Heat Mass Tranfer 52 (2009) 1337–1352.
[17] R.K. Shah, A.L. London, Laminar Flow Forced Convection in Ducts – A Source Book for Compact Heat Exchanger Analytical Data. Academic Press, New York, 1978.
[18] Z.Y. Guo, Z.X. Li, Size effect on single-phase channel flow and heat transfer at microscale. Int. J. Heat Fluid Flow 24 (2003) 284–298.
[19] Y. Bayazitoglu, S. Kakaç, Flow regime in microchannel single-phase gaseous fluid flow. in: S. Kakaç, L. Vasiliev, Y. Bayazitoglu, Y. Yener (Eds.), Microscale Heat Transfer—Fundamentals and Applications. Kluwer Academic Publishers, The Netherlands, 2005.
[20] W. Sun, S. Kakaç, A.G. Yazicioglu, A numerical study of single-phase convective heat transfer in microtubes for slip flow. Int. J. Thermal Sci. 46 (2007) 1084–1094.
[21] C. Nonino, S. Del Giudice, S. Savino, Temperature dependent viscosity effects on laminar forced convection in the entrance region of straight ducts. Int. J. Heat Mass Tranfer 49 (2006) 4469–4481.
[22] V. Kumar, P. Gupta, K.D.P. Nigam, Fluid flow and heat transfer in curved tubes with temperature-dependent properties. Ind. Eng. Chem. 46 (2007) 3226–3236.
[23] Z. Li, X. Huai, H. Tao, H. Chen, Effects of thermal property variations on liquid flow and heat transfer in microchannel heat sinks. App. Thermal Eng. 27 (2007) 2803–2814.
[24] K.C. Toh, X.Y. Chen, J.C. Chai, Numerical computation of fluid flow and heat transfer in microchannels. Int. J. Heat Mass Tranfer 45 (2002) 5133–5141.
[25] D. Bradley, A.G. Entwistle, Developed laminar flow heat transfer from air for variable physical properties. Int. J. Heat Mass Tranfer 8 (1965) 621–638.
[26] S. Kakaç, The effect of temperature-dependent fluid properties on convective heat transfer. in: S. Kakaç, R.K. Shah, W. Aung (Eds.), Handbook of Single-Phase Convective Heat Transfer. Wiley, New York, 1987, pp. 18.1–18.8.
[27] H. Herwig, M. Voigt, F.J. Bauhaus, The effect of variable properties on momentum and heat transfer in a tube with constant wall temperature. Int. J. Heat Mass Tranfer 32 (1989) 1907–1915.
[28] S.P. Mahulikar, H. Herwig, Theoretical investigation of scaling effects from macro-to-microscale convection due to variations in incompressible fluid properties. Appl. Phys. Lett. 86 (2005) 1–3.
[29] S.P. Mahulikar, H. Herwig, Physical effects in laminar micro-convection due to variations in incompressible fluid properties. Phys. Fluids 18 (2006) 1–12.
[30] S.P. Mahulikar, H. Herwig, O. Hausner, F. Kock, Laminar gas micro-flow convection characteristics due to steep density gradients. Europhys. Lett. 68 (2004) 811–817.
[31] H. Herwig, S.P. Mahulikar, Variable property effects in single-phase incompressible flows through microchannels. Int. J. Therm. Sci. 45 (2006) 977–981.
[32] S.P. Mahulikar, H. Herwig, Physical effects in pure continuum-based laminar micro-convection due to variations of gas properties. J. Phys. D: Appl. Phys. 39 (2006) 4116–4123.
[33] N.P. Gulhane, S.P. Mahulikar, Variation in gas properties in laminar micro-convection with entrance effect. Int. J. Heat Mass Tranfer 52 (2009) 1980–1990.
[34] R.B. Bird, W.E. Stewart, E.N. Lightfoot, Transport Phenomena Appendix B, second ed. Wiley, New York, 2002, pp. 310–315.
[35] E.R.G. Eckert, R.M. Drake Jr., Analysis of Heat and Mass Transfer. Hemisphere, Washington, 1987.
[36] J.D. Anderson Jr., Hypersonic and High Temperature Gas Dynamics. McGraw-Hill, Singapore, 1989, pp. 605–608.
[37] S.P. Mahulikar, C.P. Tso, A new classification for thermal development of fluid flow in a circular tube under laminar forced convection. Proc. R. Soc.. (Lond.), (Ser. A): Math., Phys. Eng. Sci. 458 (2002) 669–682.
[38] H.R. van den Berg, C.A. ten Seldam, P.S. van der Gulik, Compressible laminar flow in a capillary. J. Fluid Mech. 246 (1993) 1–20.
[39] G.P. Celata, M. Cumo, V. Marconi, S.J. Mcphail, G. Zummo, Micro-tube liquid single-phase heat transfer in laminar flow. Int. J. Heat Mass Tranfer 49 (2006) 3538–3546.
[40] W. Qu, G.M. Mala, D. Li, Heat transfer for water flow in trapezoidal silicon microchannels. Int. J. Heat Mass Tranfer 43 (2000) 3925–3936.
[41] E.N. Sieder, C.E. Tate, Heat transfer and pressure drop of liquids in tubes. Ind. Eng. Chem. 28 (1936) 1429–1433.
[42] P.Y. Wu, W.A. Little, Measuring of the heat transfer characteristics of gas flow in fine channel heat exchangers for microminiature refrigerators. Cryogenics 24 (1984) 415–420.